



## SHORT COMMUNICATION

# ACTIN-RELATED PROTEIN (ARP2) INSERTS INTO ARTIFICIAL LIPID MEMBRANES

WOLFGANG H. GOLDMANN<sup>1\*</sup> and GERHARD ISENBERG<sup>2</sup>

<sup>1</sup>Renal Unit, Dept. of Medicine, Massachusetts General Hospital, Harvard Medical School, Charlestown, MA 02129, U.S.A.; <sup>2</sup>Dept. of Biophysics E22, Technical University of Munich, D-85747 Garching, Germany

Received 28 January 2002; accepted 27 July 2002

Arp2 is localized in the cytoplasm of eukaryotic cells where it controls actin dynamics. Computer analyses have suggested one possible lipid binding site, residues 185–202 of the primary amino acid sequence on Arp2, that could allow for membrane attachment/insertion. We expressed this region as a fusion protein with schistosomal glutathione S-transferase (GST) and investigated the interaction of this fragment with mixtures of dioleoylphosphatidylserine (DOPS) and dioleoylphosphatidylglycerol (DOPG) phospholipids in reconstituted lipid bilayers using differential scanning calorimetry (DSC). Calorimetric measurements showed that as the fusion protein increased, the main chain transition enthalpy decreased and the chain-melting temperature shifted, which is indicative of partial protein insertion into the hydrophobic region of the lipid membrane. This was confirmed using the Langmuir Blodgett technique (*film balance*) on lipid monolayers. The dissociation constant ( $K_d$ ) determined by the temperature jump method was approximately 1.1  $\mu$ M.

© 2002 Elsevier Science Ltd. All rights reserved.

KEYWORDS: Arp2; actin; lipid membrane.

## INTRODUCTION

The actin-related proteins (Arps) have recently been identified based on their sequence homology to conventional actin, and it has been shown that some Arps are clearly involved in cytoskeletal functions (Machesky and Gould, 1999; Pollard *et al.*, 2000; May, 2001). The Arp2/3 complex is thought to play a central role in controlling actin dynamics by its ability to nucleate actin filament assembly, to cap the pointed ends of filaments, and to cross-link filaments into networks (Mullins *et al.*, 1998; Weeds and Yeoh, 2001). To co-operate with other regulating proteins for the development

of protrusive forces, it is necessary that this complex is located at the cytoplasmic face of the plasma membrane (Condeelis, 2001).

We used computer analyses based on recent structure predictions of the primary amino acid sequence of the Arp2/3 complex and found one region on Arp2 that could facilitate lipid membrane attachments or anchoring, namely residue 185–202 (RDVTRYLIKLLLLRGYVF). This region may attach to phospholipid membranes. In this study, we expressed this region as a fusion protein attached to schistosomal GST and used lipid vesicles (DOPG/DOPS, 1:1) of ~200 nm diameter to probe its insertion into the hydrophobic region of lipid mono- and bilayers. We applied differential scanning calorimetry and film balance technique, and measured the protein's association with lipids using the temperature jump method.

\*To whom correspondence should be addressed: Massachusetts General Hospital, Bldg. 149, 13th Street, Room 8200, Charlestown, MA 02129, U.S.A. Fax: +1-617-726-5671; E-mail: [wgoldmann@partners.org](mailto:wgoldmann@partners.org)

This work is dedicated to Hannelore Karspeck on her 55th birthday.

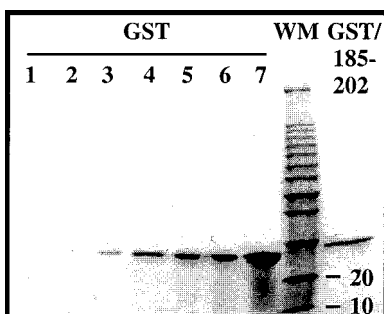


**Fig. 1. Gel chromatography** The purity of the recombinant protein was checked by a 15% analytical polyacrylamide gel. Lane 1=0.01; 2=0.05; 3=0.1; 4=0.5; 5=1.0; 6=2.0; 7=10  $\mu$ g GST. WM=molecular weight marker in (kDa). All lanes were loaded with 5  $\mu$ l protein. The purity of the expressed protein was higher than 95%, judged by densitometry.

## MATERIALS AND METHODS

### Structure prediction plots

The primary amino acid sequence of *Acanthamoeba castellanii* Arp2 was used for structure predictions, as described by Kelleher *et al.* (1995), and deposited at the GenBank Data Library, accession no. U29609 (NCBI). Briefly, to search for the average hydrophobicity and the hydrophobic moment, we constructed plots according to the method of Kyte and Doolittle (1982), using the normalized 'consensus' scale from Eisenberg *et al.* (1984) as the hydrophobicity scale for amino acids.

### Recombinant protein

Two pairs of oligonucleotides (Genosys) coding for amino acids 185–202 of the *Acanthamoeba castellanii* Arp2 sequence were annealed by the method previously described by Goldmann *et al.* (1999). The bacterial strain BL-21 (de3) was used for the expression of GST and the GST-coupled Arp2 fragment, GST/185–202. The protein transformed from BL-21 (de3) was then purified according to the procedure described by Smith and Johnson (1988). The purity was  $\geq 95\%$ , as judged by densitometry (Fig. 1).

### Lipid mono- and bilayers

Dioleoylphosphatidylserine (DOPS) and dioleoylphosphatidylglycerol (DOPG) were obtained from Avanti Polar Lipids (Birmingham, AL, U.S.A.). The phospholipids, DOPG and DOPS were dissolved in a chloroform/methanol solution of 9:1 (v/v). These lipids were then spread onto a solution containing 10 mM HEPES, 1 mM EDTA at pH

7.5, and 5–15 mM NaCl, rendering a homogeneous lipid monolayer. All bilayers were prepared by sonication followed by extrusion as described by Pêcheur *et al.* (1997). Liposomes composed of DOPG/DOPS (1 mg/ml; 1:1) had an average diameter of  $\sim 200$  nm. The phospholipid concentration was measured by the method of Bartlett (1959).

### Differential scanning calorimetry (DSC), Langmuir Blodgett (film balance), and temperature jump method

DSC samples, containing liposomes of 1 mg/ml mixed with proteins, were put into the sample cell and scans were performed at a heating rate of 30°C/h (Fig. 3A). Data analysis was carried out as previously described by Goldmann *et al.* (1992). Monolayer experiments were performed using film balance, as described schematically in Figure 4A and in detail by Tempel *et al.* (1994). In brief, the unit consists of a Langmuir trough (volume=30 ml) and a Peltier thermoelement. The fluid surface pressure was detected by a Wilhelmy system. Protein-lipid binding/insertion was achieved by the temperature jump method, as shown schematically in Figure 5A and described in detail by Goldmann and Geeves (1991). In brief, a solution containing lipids and proteins at 10°C ( $T_1$ ) was heated to 30°C ( $T_2$ ) within 150 ms. Changes in light scatter intensity were recorded and taken as a measure of protein/lipid association over time as the solution equilibrated at 30°C.

## RESULTS AND DISCUSSION

### Structure prediction plots

The predictions shown in Figure 2 were carried out as described by Tempel *et al.* (1995). The region of significant hydrophobic character is indicated around segment 185–202, and a surface-seeking character can be predicted (shown by arrows). The consensus score values are fairly high, and the probability that the amphipathic arrangement of residues occurs by chance is small. The average charge of this stretch is positive.

### Differential scanning calorimeter (DSC) measurements

Figure 3B shows the variation of the main phase transition of lipid vesicles (DOPG/DOPS at 1 mg/ml and molar ratio of 1:1) in the presence of

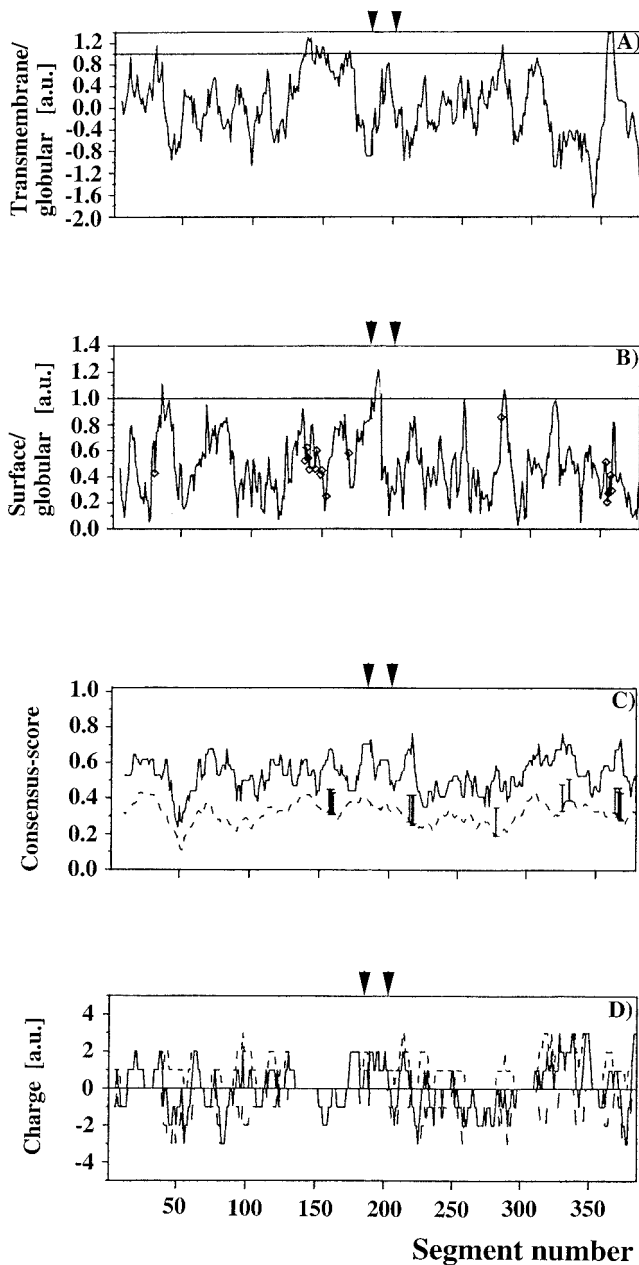


**Fig. 2.** Structure prediction plots (A) Hydrophobicity, (B) Hydrophobic moment, and (C) Probability for residues of Arp2 according to the methods described by Kyte and Doolittle (1982). Secondary structures (D) were predicted by Eisenberg *et al.* (1984). The amino acid window was 11. The arrows indicate the hydrophobic segment, 185–202. *Note:* Segment 185–202 (RDVTRYLIKLLLLRGYVF) from *Acanthamoeba castellanii* (continuous line, C+D) (GenBank accession no. U29609) shows high homology with the same segment from bovine Arp2 (dotted line, C+D) (RDITRYLIKLLLLR GYAF; accession no. 1K8K:B) (Kelleher *et al.*, 1995; Robinson *et al.*, 2001).

GST/185–202.  $T_s$  depicts the solidus line (pre-transition) and  $T_l$  the liquidus (post-transition) line of thermograms, and  $T_s^*$  and  $T_l^*$  show DOPG/

DOPS vesicles in the absence of GST/185–202 (a). With increasing concentrations of GST/185–202 (b→f), the thermotropic properties of the lipid vesicle change, which is indicative of protein-lipid interaction/insertion. Control experiments with pure GST showed no change in the thermogram compared to pure lipids.

#### Langmuir Blodgett (film balance) measurements

Figure 4B shows the time/pressure diagram as measured by the Langmuir Blodgett method. Pure DOPG/DOPS lipid layers were spread on buffer and 25  $\mu\text{g/ml}$  GST ( $\nabla$ ) or GST/185–202 ( $\Delta$ ) was injected into the subphase. The arrow indicates the time of injection. Pressure changes over time were recorded: pure GST and GST coupled to the segment 185–202 increased over 7 h from around 20 to 22 and 25 mN/m, respectively. The marked increase in lateral pressure for GST/185–202 is probably due to the insertion of the Arp2 segment into the lipid monolayer, while the slight pressure increase for pure GST may result from charged interaction with lipid headgroups. *Note:* the pressure for pure DOPG/DOPS (–) remained constant over the entire period.

#### Temperature jump measurements

Figure 5B shows the temperature-induced changes in light scatter (LS) signal of a 0.3 ml solution containing DOPG/DOPS (1 mg/ml; 1:1) and increasing concentrations of GST/185–202. The interaction with lipids was monitored at 365 nm after the T-jump ( $10^\circ\text{C} \rightarrow 30^\circ\text{C}$ ) and the traces were fitted to a single exponential. The rate of association for the reaction was calculated using the relation described by Goldmann *et al.* (1998),  $k_{\text{obs}} = k_{+1}[\text{lipid} \cdot \text{GST/185–202}] + k_{-1}$ . A plot of the observed rates against the GST/185–202 concentrations of 100, 300, 500, and 700 nM is shown in (C). The line represents the best fit to the data and gives a gradient of  $5400 \text{ M}^{-1} \text{ s}^{-1}$ , an intercept of  $0.006 \text{ s}^{-1}$ , and a  $K_d$  of 1.1  $\mu\text{M}$ . Control experiments using either pure GST or pure lipids did not change the LS signal.

The major finding in this study is that Arp2 partially inserts into artificial lipid membranes and that this attachment/insertion is of relatively high affinity. In DSC experiments, the incubation of increasing amounts of the segment 185–202 bound to GST with charged liposomes shifted the onset of the chain melting ( $T_s^* \rightarrow T_s$ ) to lower temperatures, and shifted the completion of chain melting ( $T_l^* \rightarrow T_l$ ) to higher temperatures. This behaviour

### Differential Scanning Calorimeter

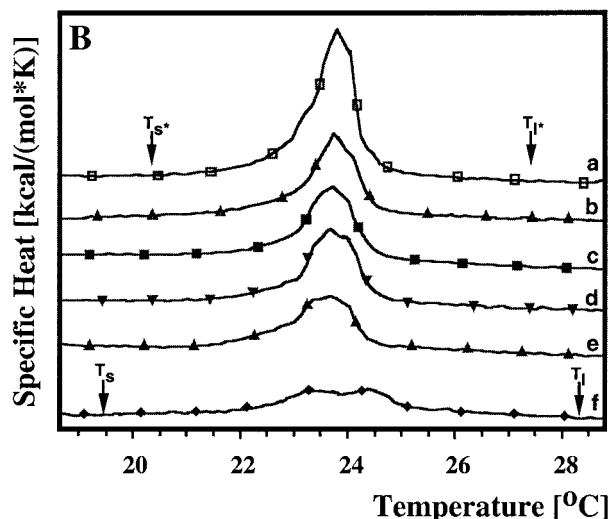
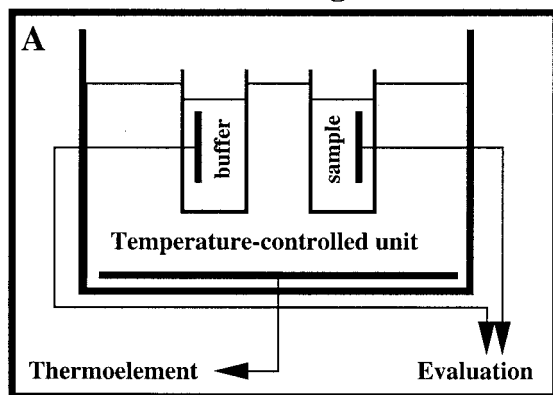


**Fig. 3.** Differential scanning calorimetry (A) Schematic diagram. (B) The endotherms show the variation of main phase transition of lipid vesicles (DOPS/DOPG at 1 mg/ml and 1:1 ratio).  $T_s^*$  and  $T_s$  indicate the solidus line and  $T_l^*$  and  $T_l$  the liquidus line of lipid vesicles in the absence and presence of GST/185–202, respectively. (a) Pure lipids; (b) 1:1500 protein/lipid; (c) 1:770; (d) 1:350; (e) 1:200; (f) 1:100. Buffer: 10 mM Hepes, 1 mM EDTA, and 5 mM NaCl at pH 7.5.

### Langmuir Blodgett Apparatus

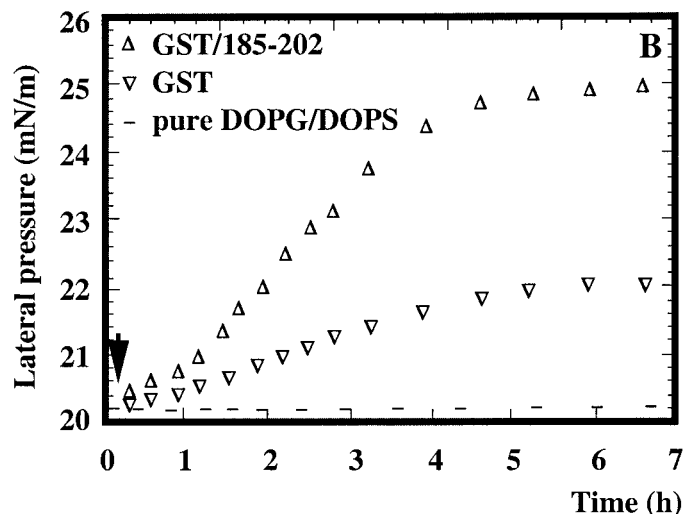
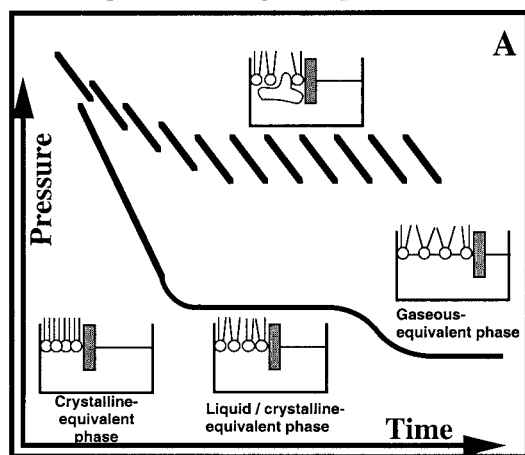


**Fig. 4.** Langmuir Blodgett apparatus (A) Schematic diagram. (B) Time/area diagram as measured by the LB technique. Pure DOPS/DOPG phospholipid monolayers were spread on buffer and 25  $\mu\text{g/ml}$  GST ( $\nabla$ ) or GST/185–202 ( $\Delta$ ) was injected into the subphase. The arrow indicates the time of injection. The pressure of  $\sim 20$  mN/m was constant for pure DOPS/DOPG (–) over 7 h. Buffer: 10 mM Hepes, 1 mM EDTA, and 5 mM NaCl at pH 7.5 and 20°C.

can be explained by two effects: (a) stabilization and condensation, and (b) expansion and rearrangement of the bilayer due to hydrophobic interaction. Two-dimensional lipid monolayers spread onto an air/water interface are ideal model systems to study the insertion and pattern formation of proteins within membranes, especially those which electrostatically adsorb to the membrane surface and penetrate only into one half of the hydrophobic lipid leaflet. Lateral pressure changes of

lipid mixtures independent of absorbed or inserted proteins after injection into the subphase allow the timely recording of Arp2 fragment insertion behaviour. At a lateral pressure of approximately 20 mN/m after protein injection at ( $t=0$ ) the pressure increases to 25 mN/m after 7 h, which is due to protein insertion into the lipid layer. Using the Gibbs energy relation, we estimated protein adsorption/insertion of roughly 0.1  $\mu\text{M}$ . We used a moderately fast temperature jump apparatus (dead

## Temperature Jump

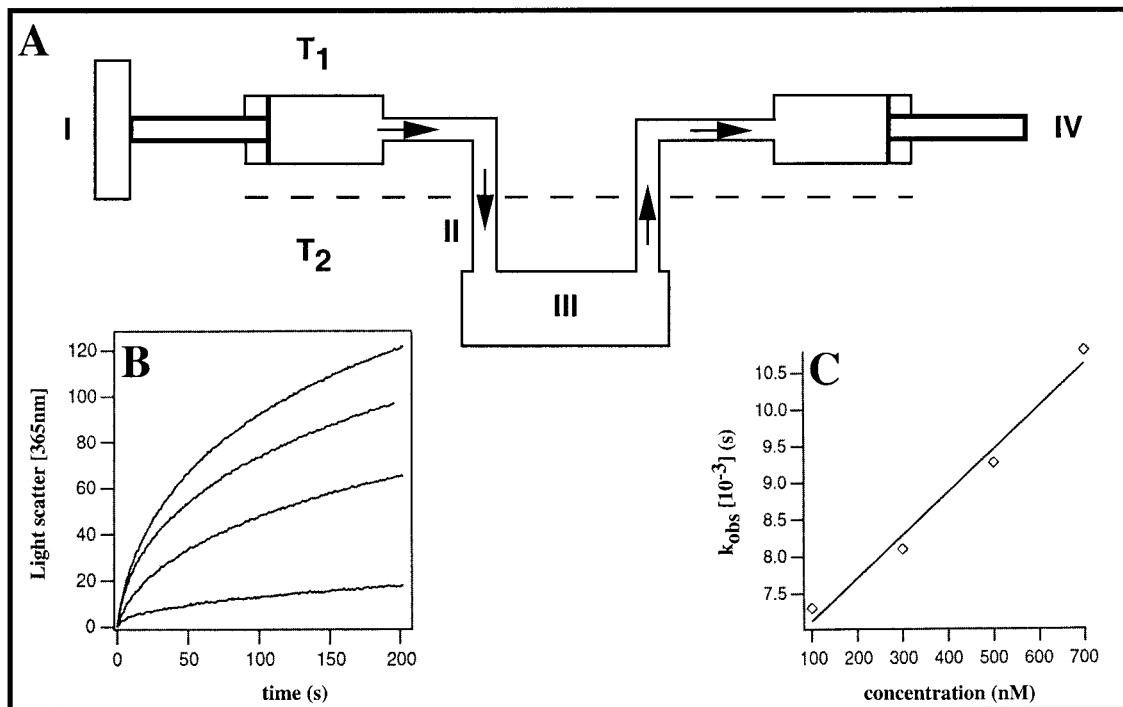


**Fig. 5.** Temperature jump apparatus (A) Schematic diagram as described by Goldmann and Geeves (1991). (I) Pressure driving ram with syringe; (II) Tubing immersed in thermostatic tank; (III) Quartz observation cell; (IV) Stopping syringe; components below the dotted line are thermostated at ( $T_2=30^\circ\text{C}$ ) and those above are at ( $T_1=10^\circ\text{C}$ ). (B) Temperature-induced changes in LS signal at 365 nm; the traces indicate an average of three experiments. (C) Plot of observed rates ( $\text{s}^{-1}$ ) against the concentration of DOPG/DOPS and GST/185–202. The line represents the best fit line to the data and the calculated  $K_d$  equals  $1.1\ \mu\text{M}$ . Conditions: temperature jump from  $10^\circ\text{C}$  to  $30^\circ\text{C}$  in approximately 150 ms at 3 bar. Buffer: 10 mM Hepes, 1 mM EDTA, and 5 mM NaCl at pH 7.5.

time  $\leq 150$  ms) to measure the association kinetics of GST/185–202 with lipids. We calculated a dissociation constant,  $K_d$  of  $1.1\ \mu\text{M}$ , which is in agreement with other cytosolic proteins, such as vinculin ( $K_d \sim 3\ \mu\text{M}$ ) and talin ( $K_d \sim 0.4\ \mu\text{M}$ ), under similar experimental conditions (Goldmann *et al.*, 1995).

In summary, our observations of the interaction of the Arp2 fragment with phospholipid membranes suggest that it may be involved, not only in actin nucleation, capping, and cross-linking in cells (Mullins *et al.*, 1998; May, 2001; Condeelis, 2001), but also in transient membrane attachment in the regulation of motility. Recent crystal structure analyses of the bovine Arp2/3 complex support our assumption of a hydrophobic region on Arp2 segment 185–202 from *Acanthamoeba castellanii* (Robinson *et al.*, 2001).

### ACKNOWLEDGEMENTS

We thank M. Tempel, J. M. Teodoridis, B. Hui, and S. Doerhoefer for their technical assistance and

Judith Feldmann, PhD for proof-reading this manuscript. This work was supported by the Deutsche Forschungsgemeinschaft (DFG) grant Is 25/8-1 and by a Collaborative Research Grant from NATO. Excerpts were presented at the 2001 ASCB meeting in Washington in poster form and published in *Mol. Biol. Cell*, **12**, 333a.

### REFERENCES

- BARLETT GR, 1959. Phosphorus assay in column chromatography. *J Biol Chem* **234**: 466–468.
- CONDEELIS J, 2001. How is actin polymerization nucleated *in vivo*? *Trends in Cell Biol* **11**: 288–293.
- EISENBERG G, SCHWARZ E, KOMAROMY M, WALL R, 1984. Analysis of membrane and surface protein sequences with the hydrophobic moment plot. *J Mol Biol* **179**: 125–142.
- GOLDMANN WH, GEEVES MA, 1991. A slow temperature jump apparatus built from a stopped-flow machine. *Anal Biochem* **192**: 55–58.
- GOLDMANN WH, NIGGLI V, KAUFMANN S, EISENBERG G, 1992. Probing actin and liposome interaction of talin and talin-vinculin complexes: a kinetic, thermodynamic, and lipid labeling study. *Biochemistry* **31**: 7665–7671.

- GOLDMANN WH, SENGER R, KAUFMANN S, ISENBERG G, 1995. Determination of the affinity of talin and vinculin to charged lipid vesicles: a light scatter study. *FEBS Lett* **368**: 516–518.
- GOLDMANN WH, GUTTENBERG Z, EZZELL RM, ISENBERG G, 1998. The study of fast reactions by the stopped-flow method. In: Isenberg G, ed. *Modern Optics, Electronics, and High Precision Techniques in Cell Biology*. Heidelberg, Springer-Verlag. 161–172.
- GOLDMANN WH, TEODORIDIS JM, SHARMA CP, HU B, ISENBERG G, 1999. Fragments from actin binding protein (ABP-280, filamin) insert into reconstituted lipid layers. *Biochem Biophys Res Comm* **259**: 108–112.
- KELLEHER JF, ATKINSON SJ, POLLARD TD, 1995. Sequence, structural models, and cellular localization of the actin-related proteins Arp2 and Arp3 from *Acanthamoeba*. *J Cell Biol* **131**: 385–397.
- KYTE J, DOOLITTLE RF, 1982. A simple method for displaying the hydrophobic character of a protein. *J Mol Biol* **157**: 105–132.
- MACHESKY LM, GOULD KL, 1999. The Arp2/3 complex: a multifunctional actin organizer. *Curr Opin Cell Biol* **11**: 117–121.
- MAY RC, 2001. The arp2/3 complex: a central regulator of the actin cytoskeleton. *Cell Mol Life Sci* **58**: 1607–1626.
- MULLINS RD, HEUSER RD, POLLARD TD, 1998. The interaction of arp2/3 complex with actin: nucleation, high affinity pointed end capping, and formation of branching networks of filaments. *Proc Natl Acad Sci USA* **96**: 6181–6186.
- PECHEUR EI, HOEKSTRA D, SAINT-MARIE J, MAURIN L, BIENVENUE A, PHILIPOT JR, 1997. Membrane anchorage brings about fusogenic properties in a short synthetic peptide. *Biochemistry* **36**: 3773–3781.
- POLLARD TD, BLANCHOIN L, MULLINS RD, 2000. Molecular mechanisms controlling actin filament dynamics in non-muscle cells. *Annu Rev Biophys Biomol Struct* **29**: 545–576.
- ROBINSON RC, TURBEDSKY K, KAISER DA, MARCHAND JB, HIGGS HN, CHOE S, POLLARD TD, 2001. Crystal structure of Arp2/3 complex. *Science* **294**: 1679–1684.
- SMITH DB, JOHNSON KS, 1988. Single-step purification of polypeptides expressed in *Escherichia coli* as fusions with glutathione S-transferase. *Gene* **67**: 31–40.
- TEMPEL M, GOLDMANN WH, DIETRICH C, NIGGLI V, WEBER T, SACKMANN E, ISENBERG G, 1994. Insertion of filamin into lipid membranes examined by calorimetric, film balance, and lipid labelling method. *Biochemistry* **33**: 12565–12572.
- TEMPEL M, GOLDMANN WH, ISENBERG G, SACKMANN E, 1995. Interaction of the 47-kDa talin fragment and the 32-kDa vinculin fragment with acidic phospholipids. *Biophys J* **69**: 228–241.
- WEEDS A, YEOH S, 2001. Action at the Y-branch. *Science* **294**: 1660–1661.